Motion Prediction for Computer-Assisted Beating Heart Surgery

Wael Bachta*, Pierre Renaud, Loïc Cuvillon, Edouard Laroche, Antonello Forgione, and Jacques Gangloff, *Member, IEEE*

***Abstract*—Off-pump totally endoscopic coronary artery bypass grafting is a milestone for cardiac surgery, and still a technical challenge. Indeed, the fast and complex cardiac motion makes this operating method technically demanding. Therefore, several robotic systems have been designed to assist the surgeons by compensating for the cardiac motion and providing a virtually motionless operating area. In the proposed systems, the servoing schemes often take advantage of a prediction algorithm that supplies the controller with some future heart motion. This prediction enlarges the control-loop bandwidth, thus allowing a better motion compensation. Obviously, improving the prediction accuracy will lead to better motion-compensation results. Thus, a current challenge in computer-assisted cardiac surgery research is the design of efficient heart-motion-prediction algorithms. In this paper, a detailed survey of the main existing prediction approaches is given and a classification is provided. Then, a novel prediction technique based on amplitude modulation is proposed, and compared with other techniques using *in vivo* collected datasets. A final discussion summarizes the main features of all the proposed approaches.**

***Index Terms*—Beating heart surgery, heart motion modeling, prediction algorithm.**

I. Introduction

CONVENTIONAL coronary artery bypass grafting (CABG) with cardiopulmonary bypass allows the surgeons to operate on a motionless heart. However, the use of a heart–lung machine is proven to cause deleterious effects on the neurological, renal, and respiratory functions [1], [2]. In order to avoid such postoperative complications, off-pump CABG has been proposed [3]: the procedure consists of operating on a beating heart. However, the complex motion of the heart makes off-pump CABG technically challenging, especially in a totally endoscopic surgery context. For example, the left anterior descending coronary artery can exhibit an excursion of 12.5 mm, whereas its diameter is about 1 mm [4]. Mechanical stabilizers are therefore designed to overcome this difficulty by locally reducing the myocardium excursion. The residual motion using current stabilizers is, however, far beyond the necessary stabilization accuracy that can be evaluated to 0.1 mm with respect to the 1–2 mm diameter of the coronary arteries and the 70 μm diameter of the stitching thread. The insufficient performance of the cardiac stabilizers is pointed out in the literature. The residual cardiac motion is evaluated in [4] and [5] through experiments on pigs, using commercially available passive stabilizers. In the first experiment, the residual anterior–posterior excursion for three pigs ranges between 0.5 and 2.6 mm using a passive Medtronic Octopus device. In the second experiment, the reported systolic to diastolic motion amplitude is about 1.5, 2.1, and 1.5 mm using, respectively, a CTS Axius Guidant Stabilizer System, a Genzyme Immobilizer, and a Medtronic Octopus. Loisance *et al.* [6] present the results of robot-assisted totally endoscopic CABG experiments on human beings. One of the reported difficulties encountered by the surgeons is the significant residual motion of the passive Medtronic EndoOctopus stabilizer during the tests. Kappert *et al.* [7] conclude that further improvement of endoscopic stabilization may improve the results they obtained during robotic-enhanced CABG.

Even with the use of a stabilizer, the frequency spectrum of the cardiac motion contains high frequencies corresponding to the harmonics of the fundamental cardiac frequency [8]. The average heart rate is about 70 beats/min, i.e., 1.16 beats/s, whereas the human tracking bandwidth is about 1 Hz [9]. The cardiac motion thus contains frequencies at the limit of and beyond the tracking abilities of surgeons.

Many contributions have been proposed in order to overcome the difficulty arising from the significant cardiac motion, sometimes even without making use of mechanical stabilization. Pioneering work was reported in [10]. The idea is to attach the surgeon's hands to a moving platform that tracks the heart motion, so that the surgical area is motionless with respect to the surgical instruments held by the surgeon. In addition, a vision system mounted on the same platform provides the surgeons with a virtually stable image of the heart. This principle is extended in [11]–[13]. In these works, a telesurgical scheme is proposed. A slave robot tracks the myocardium using high-speed visual servoing in [11] and [12], and sonomicrometry in [13]. The references given by the surgeon through the master console are superimposed to the motion-compensation subtask. A virtual stable image could also be supplied to the surgeon, as

Manuscript received November 4, 2008; revised February 13, 2009. First published June 26, 2009; current version published October 16, 2009. *Asterisk indicates corresponding author.*

*W. Bachta is with the Laboratoire des Sciences de l'Image, de l'Informatique et de la Télédétection (LSIIT), University of Strasbourg, Strasbourg 67091, France (e-mail: wael.bachta@lsiit.u-strasbg.fr).

P. Renaud is with the National Institute of Applied Science (INSA) of Strasbourg, Strasbourg 67000, France, and also with the Laboratoire des Sciences de l'Image, de l'Informatique et de la Télédétection (LSIIT), University of Strasbourg, Strasbourg 67091, France (e-mail: pierre.renaud@lsiit.u-strasbg.fr).

L. Cuvillon, E. Laroche, and J. Gangloff are with the Laboratoire des Sciences de l'Image, de l'Informatique et de la Télédétection (LSIIT), University of Strasbourg, Strasbourg 67091, France (e-mail: loic.cuvillon@lsiit.u-strasbg.fr; edouard.laroche@lsiit.u-strasbg.fr; jacques.gangloff@lsiit.u-strasbg.fr).

A. Forgione was with the Institute for Research into Cancer of the Digestive System (IRCAD)/European Institute of Tele-Surgery (EITS), University Hospitals of Strasbourg, Strasbourg 67098, France. He is now with the Advanced International Mini-Invasive Surgery (AIMS) Academy, Niguarda Càà Granda Hospital, Milan 20162, Italy (e-mail: forghy@inwind.it).

Color versions of one or more of the figures in this paper are available online at http://ieeexplore.ieee.org.

Digital Object Identifier 10.1109/TBME.2009.2026054

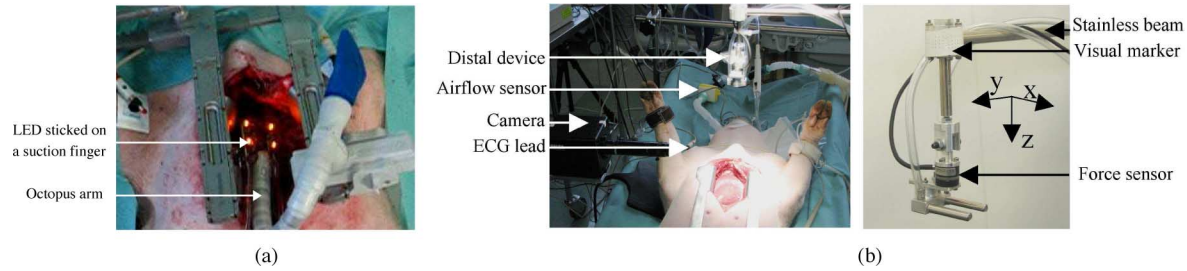

Fig. 1. Experimental setups. (a) Experimental setup for the measurement of free heart motion. (b) Experimental setup for the measurement of stabilized heart surface motion: a custom stabilizer is applied on the heart, motion is measured using high-speed vision.

in [11]. Two original approaches are proposed in [14] and [15] to overcome the problem arising from the residual motion. While, in [14], the authors have designed a miniature mobile robot that moves on the heart surface, a robotized active cardiac stabilizer which cancels the residual excursion in real time is proposed in [15].

The accuracy of any residual motion compensation scheme could be improved if the future motion is known in advance. This is why almost all the proposed approaches could take advantage of a cardiac motion prediction algorithm. This has already been investigated in [12] and [13], where model predictive control is used to enhance the myocardium tracking accuracy. Two different ways of anticipating the future heart motion are considered. The heart motion is modeled in the frequency domain in [12] by a Fourier decomposition, the obtained model allowing the prediction of future samples. A temporal modeling of the heart motion based on the ECG signal is presented in [13].

Some other prediction algorithms have been proposed in the literature. The main difference between all the approaches lies in the modeling of the cardiac motion. A frequency model similar to the one proposed in [12] is given in [8]. The estimation of the model parameters is achieved by using a derivation of the Fourier linear combiner (FLC) algorithm. A model-free prediction scheme of the heart motion is given in [16]. A linear parameter varying model of the heart motion is assessed in [17]. This model allows us to take into account the coupling between the respiratory and heartbeat components of the cardiac motion: the shape of the heartbeat component is modulated by the respiratory one. More recently, a prediction method based on an autoregressive (AR) model has been developed in [18]. A new method based on amplitude modulation is also briefly described in [19], and extended in this paper.

In this paper, a classification and a detailed review of the different techniques for heart motion prediction is proposed. Beyond this survey, we particularly outline a novel prediction algorithm based on amplitude modulation (AM), motivated by experimental observations. *In vivo* data, collected during experiments on pigs, are used to compare the most relevant approaches and discuss their accuracy.

The remainder of the paper is organized as follows. First, the properties of the heart motion already studied in the literature are recalled in Section II. Then, a review of the existing methods is given in Section III. In Section IV, the novel amplitude modulation method is described. The prediction accuracy of the different techniques is then evaluated in Section V using *in vivo* collected data. Finally, a discussion on the results and the main properties of the prediction algorithms is given in Section VI.

II. Heart Motion Properties

In this section, the main properties of the heart motion, already studied in [11], [16], and [20] are briefly recalled by analyzing *in vivo* data collected on pigs. These data will later be used for evaluation purposes. The experimental setups used for acquisition are first described.

A. In Vivo Data Collection

In vivo data are acquired during experiments on two pigs that underwent a sternotomy after receiving a general anesthesia. The pigs are under artificial ventilation.

In the first experiment [17], the heart motion is measured due to the tracking of four LEDs in the image of a 500-Hz Dalsa CAD6 high-speed camera equipped with a 50-mm lens. The LEDs are located on the suction fingers of an Octopus v4.3 stabilizer from Medtronic [see Fig. 1(a)]. The Octopus arm is unlocked so that the free motion of the myocardium is acquired. The 3-D displacement is derived from the image measurements with a modified Dementhon algorithm [21]. The measurement uncertainties of this localization system are equal to 2.6, 2.1, and 167.1 μm, respectively, along the x-, y-, and z-axes. These axes correspond approximately to the inferior–superior (IS) direction, the left–right (LR) direction, and the anterior–posterior (AP) direction.

The second dataset is acquired during another experiment under similar conditions. A custom rigid stabilizer, held by a medical robot with a high mechanical stiffness, is used to locally reduce the heart motion [15]. This stabilizer is composed of a 10-mm-diameter stainless steel beam and a distal device to have an easy access to the thoracic cavity [see Fig. 1(b)]. In Fig. 1(b), the x-, y-, and z-axes, respectively, represent the IS, LR, and AP directions. The LR direction corresponds to the stabilizer beam axis; therefore, the displacement in this direction is negligible and the heart displacement is constrained in the plane defined by the AP and IS directions. The residual displacement is measured using the position of one visual marker in the image of a 333-Hz Dalsa CAD6 high-speed camera. A Navitar Precise Eye zoom lens is used to get a resolution of 128 pixels/mm. In this experiment, the camera is positioned so that the image plane is parallel to the visual marker displacement plane. No 3-D

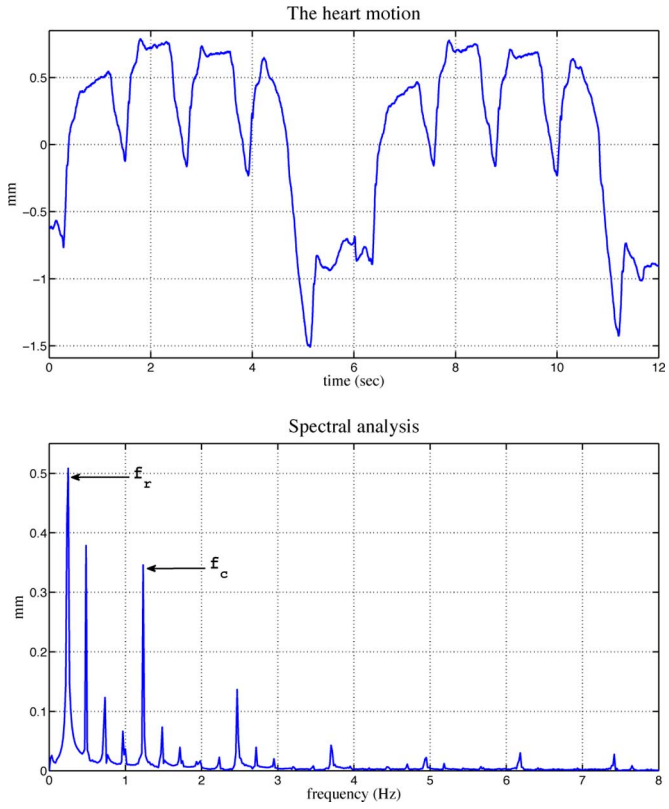

Fig. 2. Motion in the IS direction for the first dataset: temporal evolution and spectral analysis.

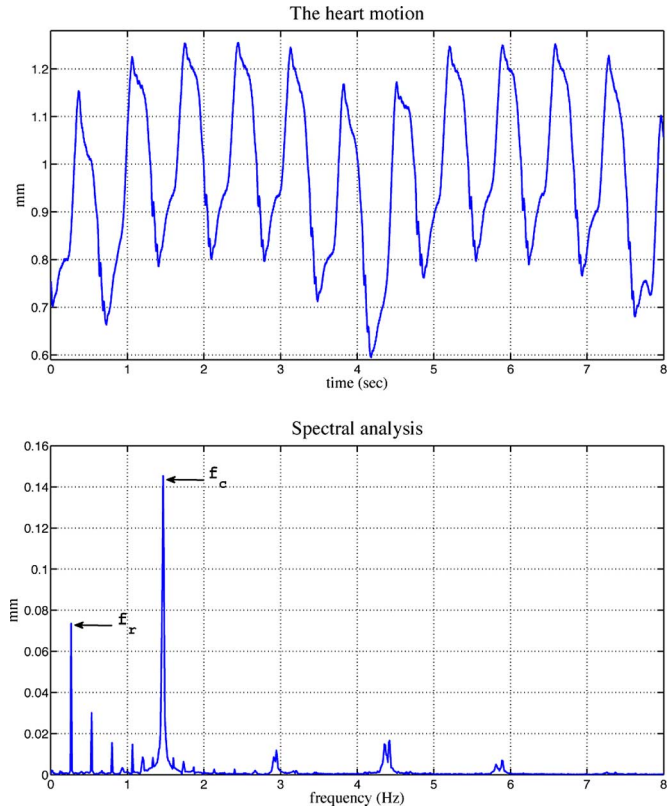

Fig. 3. Motion in the AP direction for the second dataset: temporal evolution and spectral analysis.

reconstruction is then required. The distal device is equipped with two suction fingers (Fig. 1) and encloses an ATI Nano17 force sensor. The measurement uncertainties related to this system are equal to 0.8 and 1.9 μm, respectively, along the x- and z-axes.

In both experiments, ECG and ventilation signals are acquired synchronously with motion. The ventilation is acquired through two unidirectional Honeywell Awm700 airflow sensors. The ECG signal is acquired using a three-lead ECG cable and a Schiller Cardiovit AT-6 electrocardiograph. All the data acquisitions are synchronized with the camera frame rate due to a dedicated software running under a real-time operating system.

B. Data Analysis

For the sake of clarity, only two displacement curves are represented in Figs. 2 and 3. These two figures show temporal plots and spectral analyses of, respectively, the free heart motion in the IS direction collected during the first experiment and the stabilized heart motion in the AP direction obtained with the second dataset. The two temporal plots correspond to two respiratory periods. The other measurements present the same characteristic features.

It has already been reported in [8], [12], [13], and [20] that the cardiac motion is composed of two periodic components. The slow component is due to the ventilation and the faster one corresponds to the heartbeats. The sharp transients of the heart motion correspond to the high-frequency harmonics of the heartbeat. In the remaining part of the paper, the heartbeat part of the motion will be called "heartbeat component" and denoted by $\mathcal{M}_c$. The ventilation part will be called the "respiratory component" and denoted by $\mathcal{M}_r$.

The heartbeat and ventilation frequencies can be obtained online using ECG and airflow measurements. For the first dataset corresponding to a free heart motion, the average heartbeat and ventilation frequencies are, respectively, $f_c = 1.23$ Hz and $f_r = 0.24$ Hz. For the second dataset corresponding to a stabilized heart motion, the two frequencies are, respectively, $f_c = 1.44$ Hz and $f_r = 0.26$ Hz.

III. Literature Review

The motion prediction problem consists of estimating the future heart motion based on past observations. In the literature, two families of prediction algorithms can be found: model-free (MF) and model-based approaches. The model-based approaches are dominant among the proposed prediction algorithms.

Hereafter, the most relevant MF prediction method [16] is first presented. Then the model-based approaches are studied in detail. In this paper, we consider that the prediction is used for robot control purposes. Only real-time compatible algorithms are therefore described. Modeling methods deriving the global macroscopic behavior of the heart from a microscopic modeling of the cardiac activity, as the ones presented in [22] and [23], are not under the scope of this study.

A. Model-Free Approach

The presented MF approach is developed and described in [16]. Neither *a priori* knowledge nor an explicit model of the heart motion are assumed to be known. The underlying theory of this method is based on the Takens theorem [24]. This theorem demonstrates that under certain conditions, the reconstruction of system dynamics is possible by using an embedding vector made of output measurements.

An embedding vector $\mathbf{M}_k$ computed at sample k is a sufficiently long vector made of p past measurements of the heart motion $\mathcal{M}$, sampled with a fixed period of h time samples (h and p have to be chosen appropriately). This vector can be written as

$$\mathbf{M}_k = \big[\mathcal{M}(k)\,\mathcal{M}(k-h)\cdots\mathcal{M}\big(k-(p-1)h\big)\big]^T. \quad (1)$$

Computing the prediction of the heart motion at sample $k+n$ consists of finding a previous embedding vector $\mathbf{M}_{k'}$ similar to $\mathbf{M}_k$. Then, the expected motion can be written as

$$\hat{\mathcal{M}}(k+n) = \mathcal{M}(k'+n). \quad (2)$$

A number P of previous embedding vectors similar to the current one are taken into account to compute the expectation in [16]. This allows to improve the robustness with respect to the measurement noise.

Once P embedding vectors $\mathbf{M}_{k-f_j}$ $(j=1,\ldots,P)$ presenting the best match with $\mathbf{M}_k$ are selected in a storage memory, the expected motion is defined as follows:

$$\hat{\mathcal{M}}(k+n) = \frac{1}{\sum_{j=1}^{P}(1/\delta_j)}\sum_{i=1}^{P}\frac{1}{\delta_i}\mathcal{M}(k-f_i+n) \quad (3)$$

where f_i denotes the position of the embedding vectors among the P selected ones and

$$\delta_i = \|\mathbf{M}_k - \mathbf{M}_{k-f_i}\|_2. \quad (4)$$

The algorithm can be used to predict the motion of a single landmark or generalized to process several landmarks [16]. Indeed, using several landmarks is reported to improve the robustness and reinforces the validity of the prediction if one landmark is occluded for a short time.

Another extension that improves the quality of the prediction is to take into account the correlation between the heart motion and the physiological signals, i.e., ventilation pressure and ECG. These two signals are included in the prediction scheme as additional landmarks.

B. Model-Based Approaches

Model-based approaches are usually based on a parametric model that mimics the heart motion. The model parameters are estimated recursively online using current and past motion observations. The updated model is then used to predict the motion some given steps ahead.

The issues with prediction algorithms design are twofold. First of all, an appropriate mathematical model of the heart motion has to be selected. It must be realistic enough to take into account the main characteristics of the heart motion, and it must remain compatible with a real-time use. Then, online estimation of the mathematical model parameters must be achieved using heart motion data. Attention must be paid to the estimation algorithm convergence rate, its robustness with respect to the measurement noise, and its response time when the parameters vary.

In this paper, only the first aspect, i.e., the modeling issue, is highlighted and discussed. The parameter-estimation methods are also described, but without extended discussion on the adaptive filtering theory.

In the literature, the proposed heart motion models differ by the way they use the repetitive nature of the heart motion. For some models, this property is explicitly taken into account by the model equations. In other cases, the model only considers that the current heart motion is correlated with past observations, but no explicit repetitiveness appears in the mathematical modeling. The first kind of models will be called "prior-knowledge"-based models. The second kind will be called "no prior knowledge."

1) "No Prior-Knowledge"-Based Models: In the literature, we found only one nonphenomenological modeling of the heart motion. This method, developed in [18] in order to predict the heartbeat component, is based on an AR model. In this paper, the respiratory component is neither modeled nor predicted. Indeed, the controller implemented by the authors filters this low-frequency component by means of a feedback loop. The heartbeat component $\mathcal{M}_c(k)$ at sample k is considered to be a weighted sum of the p past observations and a white noise $\mathcal{N}$

$$\mathcal{M}_c(k) = \sum_{i=1}^{p} w_i\mathcal{M}_c(k-i) + \mathcal{N}(k) \quad (5)$$

where w_i is the weight associated with the ith past observation. This equation can be expressed in a matrix form as follows:

$$\begin{aligned}\mathbf{X}_k &= \mathbf{W}\,\mathbf{X}_{k-1} + \mathbf{N}_k\\ \mathcal{M}_c(k) &= \mathbf{C}\,\mathbf{X}_k\end{aligned} \quad (6)$$

with

$$\begin{aligned}\mathbf{X}_k &= [\mathcal{M}_c(k) \quad \mathcal{M}_c(k-1) \quad \ldots \quad \mathcal{M}_c(k-(p-1))]^T\\ \mathbf{X}_{k-1} &= [\mathcal{M}_c(k-1) \quad \mathcal{M}_c(k-2) \quad \ldots \quad \mathcal{M}_c(k-p)]^T\\ \mathbf{N}_k &= [\mathcal{N}(k) \quad \mathcal{N}(k-1) \quad \ldots\mathcal{N}(k-(p-1))]^T\\ \mathbf{C} &= [1 \quad \underbrace{0 \quad \ldots \quad 0}_{p-1}]^T\end{aligned} \quad (7)$$

and

$$\mathbf{W} = \begin{pmatrix} w_1 & w_2 & \ldots & w_{p-1} & w_p\\ 1 & 0 & \ldots & 0 & 0\\ 0 & 1 & & 0 & 0\\ \vdots & & \ddots & & 0\\ 0 & 0 & \ldots & 1 & 0\end{pmatrix}. \quad (8)$$

The weights w_i, $i \in [1,p]$, represent the parameters of the heartbeat component model that have to be estimated to solve the following problem:

$$\mathcal{M}_c(k) = [w_1\,w_2\,\cdots\,w_p]\,\mathbf{X}_{k-1}. \quad (9)$$

The estimation is obtained using a recursive least square (RLS), as described in Appendix A.

Using this AR model, the prediction of the heartbeat motion n samples ahead, denoted by $\hat{\mathcal{M}}_c(k+n)$, is given by the expectation of the state equation (6) at sample $k+n$:

$$\hat{\mathcal{M}}_c(k+n) = \mathbf{C}\,\mathbf{W}^n\,\mathbf{X}_k. \tag{10}$$

Equation (10) assumes that successive samples of the heart motion are linearly dependent. Indeed, the same vector of parameters is used for all the predictions along the prediction horizon. This assumption is partially relaxed by Franke *et al.* [25]. In this paper, the prediction equation is written as

$$\begin{bmatrix} \hat{\mathcal{M}}_c(k+1) \\ \hat{\mathcal{M}}_c(k+2) \\ \vdots \\ \hat{\mathcal{M}}_c(k+n) \end{bmatrix} = \begin{bmatrix} \mathbf{V}_1 \\ \mathbf{V}_2 \\ \vdots \\ \mathbf{V}_n \end{bmatrix} \begin{bmatrix} \mathcal{M}_c(k) \\ \mathcal{M}_c(k-1) \\ \vdots \\ \mathcal{M}_c(k-p+1) \end{bmatrix}. \tag{11}$$

Using this formulation, each sample i in the prediction horizon can be predicted independently using a different weighting vector $\mathbf{V}_i$ of dimensions $1 \times p$. In order to estimate the vectors $\mathbf{V}_i$ used for the prediction, (11) is delayed by n samples as follows:

$$\begin{bmatrix} \mathcal{M}_c(k+1-n) \\ \mathcal{M}_c(k+2-n) \\ \vdots \\ \mathcal{M}_c(k) \end{bmatrix} = \begin{bmatrix} \mathbf{V}_1 \\ \mathbf{V}_2 \\ \vdots \\ \mathbf{V}_n \end{bmatrix} \begin{bmatrix} \mathcal{M}_c(k-n) \\ \mathcal{M}_c(k-n-1) \\ \vdots \\ \mathcal{M}_c(k-p-n+1) \end{bmatrix}. \tag{12}$$

Since all the motion components are known, an RLS algorithm can be used to estimate the different vectors $\mathbf{V}_i$, $i \in [1, n]$.

The authors mentioned that the filter order p is a function of the number of harmonics of the estimated signal. Indeed, they propose to model each harmonic considered in the signal by a second-order filter. Thus, the filter order could be chosen equal to twice the number of significant harmonics of the heartbeat component. Due to this tuning clue, the method could be considered as a "prior knowledge" method. But as we will see later, this tuning rule may not be always valid in practice when dealing with a noisy data. We therefore classify this method as a "no prior knowledge" one.

2) "Prior-Knowledge"-Based Models: Within this category, models take advantage of the *a priori* knowledge on the frequency content of the cardiac motion. As mentioned in Section II, the heart motion is composed of two periodic components: $\mathcal{M}_r$ and $\mathcal{M}_c$. $\mathcal{M}_r$ is due to the respiration while $\mathcal{M}_c$ is due to the heartbeats. The whole motion is written as

$$\mathcal{M}(k) = \mathcal{M}_c(k) + \mathcal{M}_r(k). \tag{13}$$

Differences between the "prior-knowledge"-based models lie in the modeling of the two components. Some authors adopt a frequency-domain modeling, using a Fourier representation, while others use temporal models.

a) Frequency domain models: Two frequency-domain prediction algorithms are proposed in [8] and [12]. In both cases, the model is based on the periodicity property of $\mathcal{M}_c$ and $\mathcal{M}_r$. Let f_c and f_r be the frequencies of the heartbeat and ventilation signals, respectively. The variables ϕ_c and ϕ_r are the associated phases. Denoting by T_s the sampling period, these phases are updated at each sample k as follows:

$$\begin{cases} \phi_c(k) = \phi_c(k-1) + 2\pi f_c T_s \\ \phi_r(k) = \phi_r(k-1) + 2\pi f_r T_s. \end{cases} \tag{14}$$

Because of their periodicity, the respiratory and heartbeat components can be modeled by truncated Fourier series

$$\hat{\mathcal{M}}_r(k) = \sum_{i=1}^{n_r} \Big(a_{ri} \sin\big(i\phi_r(k)\big) + b_{ri} \cos\big(i\phi_r(k)\big) \Big) \tag{15}$$

and

$$\hat{\mathcal{M}}_c(k) = \sum_{i=1}^{n_c} \Big(c_{ci} \sin\big(i\phi_c(k)\big) + d_{ci} \cos\big(i\phi_c(k)\big) \Big) \tag{16}$$

where n_r and n_c are, respectively, the number of relevant respiratory and heartbeat harmonics, and a_{ri}, b_{ri}, c_{ci}, and d_{ci} are the Fourier coefficients.

The FLC algorithm is used in [8] to estimate the Fourier coefficients of the two motion components. If the frequency f of a periodic signal $\mathcal{S}$ is known, the FLC algorithm allows the estimation of its Fourier coefficients. The signal can be written as follows if only the first n harmonics are taken into account:

$$\hat{\mathcal{S}}(k) = \sum_{i=1}^{n} \Big(a_i \sin\big(i\phi(k)\big) + b_i \cos\big(i\phi(k)\big) \Big) \tag{17}$$

where $\phi(k)$ is the signal phase.

Let us denote the Fourier coefficients vector $\mathbf{W}$ as

$$\mathbf{W} = \begin{bmatrix} a_i \\ b_i \end{bmatrix}_{i=1,\ldots,n}$$

and

$$\mathbf{\Phi}(k) = \begin{bmatrix} \sin\big(i\phi(k)\big) \\ \cos\big(i\phi(k)\big) \end{bmatrix}_{i=1,\ldots,n}.$$

At each sample k, the vector $\mathbf{W}$ is updated using the following equations [26]:

$$\begin{aligned} \epsilon(k) &= S(k) - \mathbf{\Phi}^T(k)\mathbf{W}(k) \\ \mathbf{W}(k+1) &= \mathbf{W}(k) + 2\mu_1 \mathbf{\Phi}(k)\epsilon(k) \end{aligned} \tag{18}$$

where μ_1 is an adaptation gain.

The FLC algorithm given before can be modified in order to estimate the frequency f also. The modified algorithm is called weighted frequency FLC (WFLC). The frequency can be estimated using the following equation:

$$f(k+1) = f(k) + 2\mu_0\epsilon(k) \sum_{i=1}^{n} i(a_i \sin\big(i\phi(k)\big) - b_i \cos\big(i\phi(k)\big)) \tag{19}$$

where μ_0 is an adaptation gain.

In the FLC algorithm, the adaptation gain μ_1 can also be modified online, using the squared estimation error

$$\mu_1(k+1) = \alpha\mu_1(k) + \beta\epsilon^2(k) \tag{20}$$

with $0 < \alpha < 1$ and $\beta > 0$. This modified FLC algorithm is called adaptive FLC (AFLC).

Both the WFLC and the AFLC are used in [8] to estimate the Fourier coefficients of the heart motion. First, the acquired motion is used as the input of an AFLC algorithm centered on the breathing frequency. This allows the estimation of the Fourier coefficients of the respiration motion model. The error resulting from the earlier estimation is then used in a second step as the input of a WFLC, in order to estimate the parameters of the heartbeat component. The combination of the AFLC and the WFLC is called tiered Fourier linear combiner (TFLC).

Using $\mathbf{W}_c(k)$ and $\mathbf{W}_r(k)$, the estimated parameter vectors of, respectively, the heartbeat and respiratory components, the expected heart motion at sample $k+n$ can be written as

$$\hat{\mathcal{M}}(k+n) = \mathbf{\Phi}_c^T(k+n)\mathbf{W}_c(k) + \mathbf{\Phi}_r^T(k+n)\mathbf{W}_r(k) \quad (21)$$

where

$$\mathbf{\Phi}_c(k) = \begin{bmatrix} \sin\big(i\phi_c(k)\big) \\ \cos\big(i\phi_c(k)\big) \end{bmatrix}_{i=1,\ldots,n_c}$$

and

$$\mathbf{\Phi}_r(k) = \begin{bmatrix} \sin\big(i\phi_r(k)\big) \\ \cos\big(i\phi_r(k)\big) \end{bmatrix}_{i=1,\ldots,n_r}.$$

The same heart motion model is considered in [12]. However, a different estimation and prediction technique is used. Indeed, an adaptive filter first estimates the heartbeat component from the measured motion. All the n_c harmonic coefficients are estimated separately. Denoting by $\hat{\mathcal{M}}_{ci}$ the estimation of the ith heartbeat harmonic, using (16), we can write

$$\hat{\mathcal{M}}_{ci}(k) = c_{ci}\sin\big(i\phi_c(k)\big) + d_{ci}\cos\big(i\phi_c(k)\big). \quad (22)$$

Coefficients c_{ci} and d_{ci} are updated using the following law [27]:

$$\begin{aligned} c_{ci}(k+1) &= c_{ci}(k) - gT_s\sin\big(i\phi_c(k)\big)\hat{\mathcal{M}}_r(k) \\ d_{ci}(k+1) &= d_{ci}(k) - gT_s\cos\big(i\phi_c(k)\big)\hat{\mathcal{M}}_r(k) \end{aligned} \quad (23)$$

with $g = 2\pi f_c/(10T_s)$.

The respiratory component estimation $\hat{\mathcal{M}}_r(k)$ is obtained by subtracting the estimated heartbeat component, which is the sum of all the harmonics, from the whole measured excursion

$$\hat{\mathcal{M}}_r(k) = \mathcal{M}(k) - \hat{\mathcal{M}}_c(k). \quad (24)$$

The prediction is then based on the periodicity of the two components and expressed in the time domain. The expected motion at sample $k+n$ is written as

$$\hat{\mathcal{M}}(k+n) = \mathcal{M}_c(k - T_c + n) + \mathcal{M}_r(k - T_r + n) \quad (25)$$

where T_c and T_r are, respectively, the floors of $1/(T_s f_c)$ and $1/(T_s f_r)$.

A similar method in the context of the mitral valve repair surgery has been recently proposed in [28]. This method is based on a Fourier decomposition of the heart motion. The Fourier coefficients are estimated using an extended Kalman filter.

The approaches proposed in [8] and [12] use the same heart model. However, two different estimation methods are considered. Since the goal of this paper is to compare the heart models rather than the estimation algorithms, the two proposed approaches are considered identical from a modeling point of view and designated as the FLC approach.

b) Temporal models: Only the heartbeat component is predicted in [13] as in [18]. The respiratory component is supposed to be canceled by a low-bandwidth tracking system. In this method, called the "last cycle" method, the heartbeat motion is considered periodic

$$\mathcal{M}_c(k) = \mathcal{M}_c(k - T_c). \quad (26)$$

Therefore, the expected motion at sample $k+n$ can simply be written as

$$\hat{\mathcal{M}}_c(k+n) = \mathcal{M}_c(k - T_c + n). \quad (27)$$

However, the authors notice that the heart motion is only quasi-periodic, i.e., small variations are observed from one heartbeat period to another. Let $\epsilon(k)$ be the difference between the current heartbeat motion measurement and the corresponding value during the past heartbeat cycle. It can be written as

$$\epsilon(k) = \mathcal{M}_c(k) - \mathcal{M}_c(k - T_c). \quad (28)$$

A method is proposed to decrease this difference gradually over the prediction horizon N by using a weighting function $f(n)$. The chosen function is a polynomial given by

$$f(n) = 1 - \left(\frac{n}{N}\right)^p \quad (29)$$

where p is the order of the correction function.

Based on (27) and the correction function f, the proposed new prediction equation for sample $k+n$ can be written as [18]

$$\hat{\mathcal{M}}_c(k+n) = \mathcal{M}_c(k - T_c + n) + f(n)\epsilon(k). \quad (30)$$

Such a prediction law can decrease the impact of heart motion variability from one period to another. However, it does not take into account the variation of the heart period itself. In order to overcome this weakness, the authors propose to use the ECG signal in order to update the heart period at each detection of the QRS complex (a combination of three electric waves, denoting the beginning of the cardiac cycle), rather than using a constant period.

A temporal modeling of the heart motion is also adopted in [17]. The method is called linear parameter varying (LPV) method. First, a separation of respiratory and heartbeat components is achieved using a gating technique. Indeed, the QRS complexes of the ECG signal are used as a clock to sample the heart motion. The heart is almost at rest during the second half of the heartbeat cycle. If the heart motion is sampled using the QRS clock delayed by half a cardiac period, then only the respiratory motion is observed, and the obtained samples represent the respiratory motion for different respiratory volumes. These samples are interpolated by a smoothing cubic spline function $\mathcal{F}$. Therefore, the respiratory motion can be reconstructed at each sample

$$\hat{\mathcal{M}}_r(k) = \mathcal{F}(k - k_{\mathrm{resp}}) \quad (31)$$

where k_{resp} is the sample number representing the beginning of the current respiratory cycle.

Then, this motion is subtracted from the whole motion to obtain the heartbeat component

$$\hat{\mathcal{M}}_c(k) = \mathcal{M}(k) - \hat{\mathcal{M}}_r(k). \tag{32}$$

The heartbeat component is modeled by a finite-impulse response (FIR) to the QRS complex considered as an impulse. The heartbeat motion at sample k can, therefore, be written as a convolution product

$$\hat{\mathcal{M}}_c(k) = l(k) * \mathrm{QRS}(k) \tag{33}$$

where $l(i)$, $i = 1, \ldots, T_c$, are the coefficients of the FIR filter.

The authors assess that the heartbeat component is quasi-periodic and modulated by the ventilation. Therefore, the coefficients of the filter representing $\mathcal{M}_c$ are considered varying and linearly dependent on the lung volume $\mathcal{V}(k)$

$$l(k) = l_0(k) + l_1(k)\mathcal{V}(k). \tag{34}$$

The filter coefficients l_0 and l_1 are identified online using an RLS algorithm.

The future heart motion is predicted using this model and the periodicity of the lung volume, due to the artificial ventilation. The expected motion at sample $k+n$ can be written as

$$\begin{aligned}\hat{\mathcal{M}}(k+n) &= \hat{\mathcal{M}}_r(k+n) + \hat{\mathcal{M}}_c(k+n) \\ &= \mathcal{F}(k - k_{\mathrm{resp}} + n) + l_0(k - k_{\mathrm{QRS}} + n) \\ &\quad + l_1(k - k_{\mathrm{QRS}} + n)\mathcal{V}(k - T_r + n)\end{aligned} \tag{35}$$

where k_{QRS} is the the sample number representing the last QRS occurrence.

IV. Amplitude Modulation Method

The authors in [17] assess the coupling between the two components of the heart motion. Indeed, the heartbeat component is proved to be dependent on the respiratory phase, and this coupling is modeled in the temporal domain. Hereafter, we propose an alternate method to take into account in a simpler way this coupling, while remaining in a Fourier coefficient estimation framework. The proposed method is mainly based on experimental observations that are first detailed.

If we zoom-in on the two spectral analysis given in Section II, we obtain plots comparable to Fig. 4. We can observe peaks that are similar to those obtained when representing the spectral content of an amplitude modulation using two periodic signals of frequencies f_c and f_r. In our case, the carrier frequency corresponds to the heartbeat frequency, and the modulating signal has the same frequency as the respiratory component. Similar observations can be made from [29, Fig. 5.24] and [18, Fig. 2]. We note that the number of modulating harmonics is lower than the number of harmonics in the respiratory component. The amplitude of these harmonics is also different from the respiratory ones. Moreover, only the first low-frequency heartbeat harmonics are modulated.

We proposed in [19] to express the cardiac motion as the sum of a respiratory component $\mathcal{M}_r$ and a heartbeat component $\mathcal{M}_c$ expressed as an AM

$$\mathcal{M}(k) = \mathcal{M}_r(k) + \mathcal{C}_c(k)(1 + \mathcal{C}_r(k)) \tag{36}$$

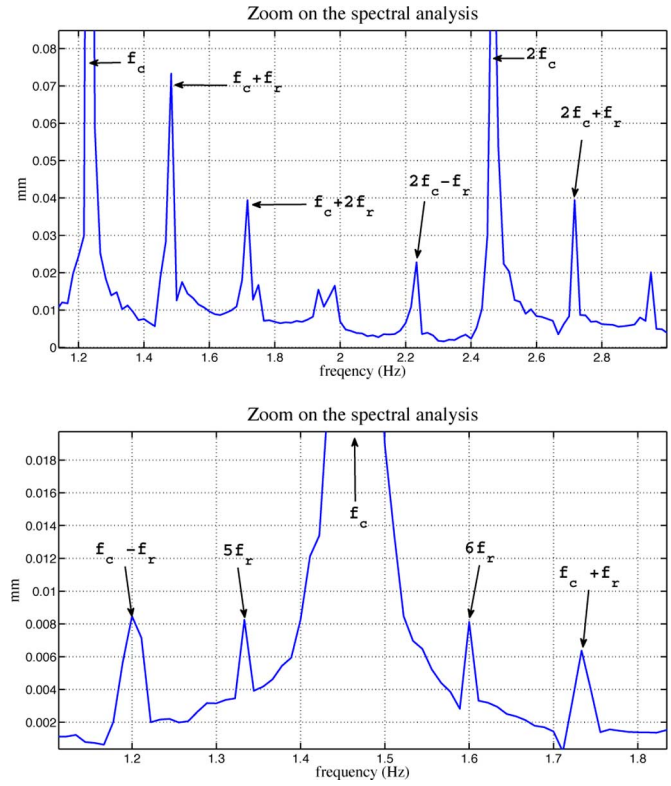

Fig. 4. Zoom on the spectral analysis of cardiac motion for the two datasets. (Top) Free heart motion (first dataset). (Bottom) Stabilized heart motion (second dataset).

where

$$\mathcal{M}_r(k) = \sum_{i=1}^{n_r} \Big(a_{ri} \sin\big(i\phi_r(k)\big) + b_{ri} \cos\big(i\phi_r(k)\big) \Big) \tag{37}$$

and $\mathcal{C}_c$ is the carrier signal representing the heartbeat fundamental frequency and its harmonics. Its Fourier decomposition can be written as follows:

$$\mathcal{C}_c(k) = \sum_{i=1}^{n_c} \Big(e_{ci} \sin\big(i\phi_c(k)\big) + f_{ci} \cos\big(i\phi_c(k)\big) \Big) \tag{38}$$

where n_c is the number of heartbeat harmonics, e_{ci} and f_{ci} are the Fourier coefficients, and $\mathcal{C}_r(k)$ is the modulating signal, which is expressed as

$$\mathcal{C}_r(k) = \sum_{i=1}^{n_r} \Big(g_{ri} \sin\big(i\phi_r(k)\big) + h_{ri} \cos\big(i\phi_r(k)\big) \Big) \tag{39}$$

with n_r being the number of respiratory harmonics, and g_{ri} and h_{ri} the Fourier coefficients.

Experimentally, the number of modulating harmonics is lower than the number of respiratory harmonics, and only the first harmonics of the heartbeat are modulated. Therefore, we rewrite $\mathcal{C}_r(k)$ as

$$\mathcal{C}_r(k) = \sum_{i=1}^{n_{r1}} \Big(g_{ri} \sin\big(i\phi_r(k)\big) + h_{ri} \cos\big(i\phi_r(k)\big) \Big) \tag{40}$$

where $n_{r1} \leq n_r$ is the number of modulating harmonics.

Moreover, (36) is rewritten as follows:

$$\mathcal{M}(k) = \mathcal{M}_r(k) + \underbrace{\mathcal{C}_c(k) + \mathcal{C}_{c1}(k)\mathcal{C}_r(k)}_{\mathcal{M}_c(k)} \tag{41}$$

where $\mathcal{C}_c$ contains all the significant heartbeat harmonics whereas $\mathcal{C}_{c1}$ contains only the first low-frequency harmonics (a truncated part of $\mathcal{C}_c$). The number of harmonics of $\mathcal{C}_{c1}$ is denoted by n_{c1}.

Hence, the heartbeat component can be expanded as follows:

$$\begin{aligned}\mathcal{M}_c = &\sum_{i=1}^{n_c}\Big(e_{ci}\sin\big(i\phi_c(k)\big) + f_{ci}\cos\big(i\phi_c(k)\big)\Big)\\ &+\sum_{i=1}^{n_{c1}}\sum_{j=1}^{n_{r1}}\Big(\underbrace{\frac{1}{2}(e_{ci}g_{rj}+f_{ci}h_{rj})}_{q_{ij}}\cos(i\phi_c(k)-j\phi_r(k))\\ &+\underbrace{\frac{1}{2}(f_{ci}h_{rj}-e_{ci}g_{ri})}_{r_{ij}}\cos(i\phi_c(k)+j\phi_r(k))\\ &+\underbrace{\frac{1}{2}(e_{ci}h_{rj}-g_{rj}f_{ci})}_{t_{ij}}\sin(i\phi_c(k)-j\phi_r(k))\\ &+\underbrace{\frac{1}{2}(e_{ci}h_{rj}+f_{ci}g_{rj})}_{v_{ij}}\sin(i\phi_c(k)+j\phi_r(k))\Big).\end{aligned} \tag{42}$$

In order to keep a linear model, all the products of terms e_{ci}, f_{ci}, g_{ri}, and h_{ri} are replaced with new terms. Using this reparametrization and (13), we can write

$$\mathcal{M}(k) = \Phi^T(k)\,\mathbf{W}(k) \tag{43}$$

where

$$\mathbf{W} = \begin{bmatrix} \begin{bmatrix} a_{ri} \\ b_{ri} \end{bmatrix}_{i=1,\ldots,n_r} \\ \begin{bmatrix} e_{ci} \\ f_{ci} \end{bmatrix}_{i=1,\ldots,n_c} \\ \begin{bmatrix} q_{ij} \\ r_{ij} \\ t_{ij} \\ v_{ij} \end{bmatrix}_{i=1,\ldots,n_{c1},\, j=1,\ldots,n_{r1}} \end{bmatrix}$$

$$\mathbf{\Phi}(k) = \begin{bmatrix} \begin{bmatrix} \sin(i\phi_r(k)) \\ \cos(i\phi_r(k)) \end{bmatrix}_{i=1,\ldots,n_r} \\ \begin{bmatrix} \sin(i\phi_c(k)) \\ \cos(i\phi_c(k)) \end{bmatrix}_{i=1,\ldots,n_c} \\ \begin{bmatrix} \cos(i\phi_c(k)-j\phi_r(k)) \\ \cos(i\phi_c(k)+j\phi_r(k)) \\ \sin(i\phi_c(k)-j\phi_r(k)) \\ \sin(i\phi_c(k)+j\phi_r(k)) \end{bmatrix}_{i=1,\ldots,n_{c1},\, j=1,\ldots,n_{r1}} \end{bmatrix}. \tag{44}$$

Using (43), the parameter vector is updated at each sample by an RLS algorithm with a forgetting factor. Prediction at sample $k+n$ can be written as

$$\hat{\mathcal{M}}(k+n) = \Phi^T(k+n)\,\mathbf{W}(k). \tag{45}$$

V. Prediction Results Comparison

In this section, the most relevant approaches are compared using the two datasets presented in Section II. These datasets correspond to a free and constrained heart motion, which allow us to consider two robotic motion compensation schemes, i.e., compensating for the whole heart motion or for the residual excursion when a cardiac stabilizer is used.

The prediction of the three motion directions is achieved simultaneously in [18]. We consider that such a coupling globally improves the results of all the proposed methods. In this section, we chose to assess the influence of heart motion modeling methods on the prediction accuracy by putting the focus on the heart motion properties. Motion in each direction is thus predicted independently from the other directions.

The "last cycle" method (Section III-B2b) is included neither in the comparison nor in Section VI. Indeed, the authors of this method also proposed the method based on an AR model (Section III-B1), and concluded that the AR-based approach gives better results than the "last cycle" method. Thus, the following methods are compared: the FLC method (Section III-B2a), the AR-based method (Section III-B1), the LPV method (Section III-B2b), the MF approach (Section III-A), and the AM method (Section IV). For a fair comparison, all the parameter estimations are achieved, when needed, using an RLS with a forgetting factor [30] (see Appendix A).

For the FLC and AM methods, all the coefficients are estimated in a single step. The two-stage method proposed in [8] gives similar results. For the AR approach [25], the respiratory component is retrieved after being estimated by an FLC algorithm. The resulting error, corresponding to the heartbeat component, is the input of the AR method.

A. Tuning Guidelines

Hereafter, some guidelines on the tuning of the parameters for the compared methods are given.

1) MF: The storage memory should be approximately equal to ten respiratory periods according to [16]. Increasing the number of embedding vectors P not only makes the algorithm more robust with respect to measurement noise, but also increases the computational cost. The variables p and h should be chosen so that an embedding vector takes into account at least one respiratory period. Increasing h yields a higher accuracy, but increases the computational cost.

2) FLC and AM: The variables n_c, n_r, n_{c1}, and n_{r1} should be set according to the signal properties. A spectral analysis can give the number of significant harmonics to take into account. The parameters are updated using an RLS algorithm with a forgetting factor. The forgetting factor λ should be chosen to have a memory horizon of at least one respiratory period: since the memory horizon is equal to $1/(1-\lambda)$ (expressed in number of samples) [31], λ should tend toward 1 when the sampling rate increases. When the measured motion is noisy, the memory horizon should be increased.

3) AR: Choosing the AR order equal to twice the number of significant harmonics in the heartbeat motion is no longer applicable when the sampling period is small and the signal

TABLE I
NUMERICAL VALUES OF PREDICTION PARAMETERS FOR TWO EVALUATED DATASETS

Method	Parameter	First data set	Second data set
MF	Storage memory size	9.6	11.2
	h	10	5
	p	400	200
	P	5	5
AR	Filter order size	400	230
	Forgetting factor	0.9999	0.9999
FLC	n_c	13	8
	n_r	4	6
	Forgetting factor	0.9999	0.9999
LPV	Smoothing factor	10^{-7}	10^{-4}
	Forgetting factor	0.9997	0.999
AM	n_c	13	8
	n_r	4	6
	n_{c1}	7	4
	n_{r1}	2	2
	Forgetting factor	0.9999	0.9999

TABLE II
ONE-HEARTBEAT-PERIOD AHEAD PREDICTION ERRORS

RMS (μm)	FLC	AR	LPV	MF	AM
First data set					
x axis	107	118	73	82	**65**
y axis	125	148	94	**59**	76
z axis	653	739	682	705	**617**
Second data set					
x axis	12	15	16	**10**	**10**
z axis	18	21	25	16	**13**

is noisy. The reader looking for some theoretical background on AR filters can refer to [32]. In this paper, the filter order was chosen by trial and error. The forgetting factor in the RLS algorithm used to identify the filter coefficients should be chosen such that the memory horizon is at least equal to one respiratory period.

4) LPV: Almost all the parameters are constrained in this method. The number of parameters defining the FIR filter is twice the number of samples of a heartbeat period, and the number of parameters defining the spline depends on the number of available points used in the interpolation. The only two parameters to tune are the smoothing factor for the spline identification and the forgetting factor used for the estimation of the FIR filter coefficients. For the choice of the smoothing factor s, the user should keep in mind that a good tradeoff between smoothing and fitting to the data is $s = 1/(1 + h^3/6)$ [33], where h is the spacing between two samples. Increasing the factor improves the fitting, and decreasing the factor improves the smoothing. The forgetting factor should be chosen such that the memory horizon is about one respiratory period.

B. Results Comparison

Prediction is achieved one heartbeat period ahead with the different approaches using the two datasets. The parameters used for each approach on the two datasets are summarized in Table I. The values are selected using the provided tuning guidelines. Prediction results are then satisfactory, but, for the sake of a fair comparison, additional trial and errors are used to optimize the performances of each algorithm.

The root mean square (RMS) of the prediction errors are summarized in Table II. The errors are computed on a time interval

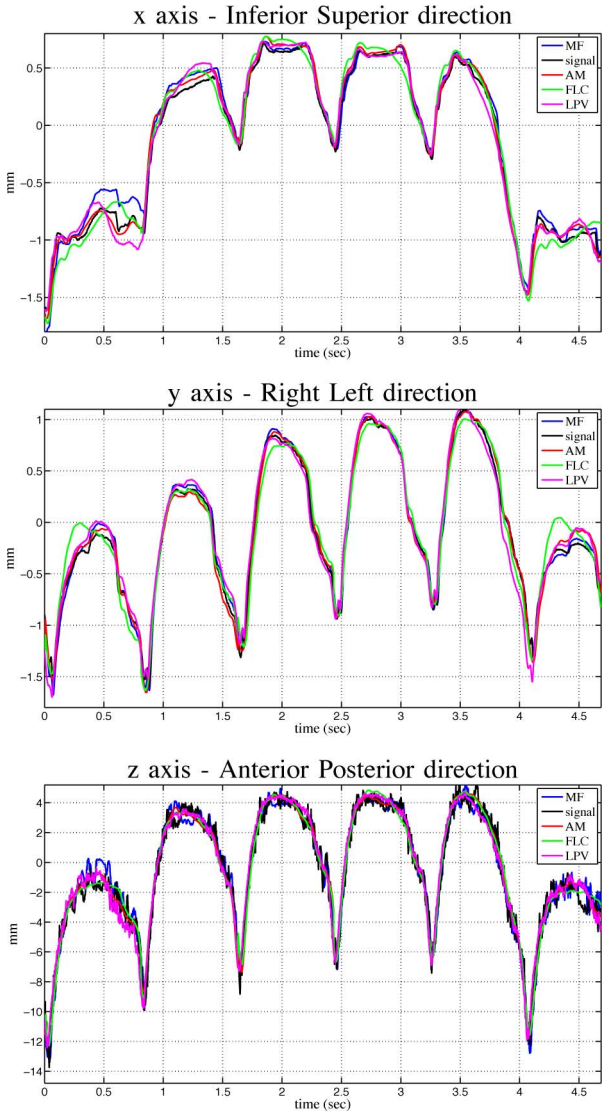

Fig. 5. First datasetone heartbeat period ahead prediction of the motion components.

of five respiratory cycles for both datasets, after prediction on ten respiratory cycles.

Figs. 5 and 6 show the prediction plots during approximately one respiratory period for the first dataset. Figs. 7 and 8 show the prediction plots for the second dataset during approximately one respiratory period. For each dataset, a separate figure is given for the AR method because the proposed algorithm handles only the heartbeat component.

VI. DISCUSSION

The discussion is centered on two points. First of all, the prediction accuracy and the tuning simplicity of the proposed approaches are discussed from a user point of view. Then, the ability of the different approaches to handle the two main characteristics of the heart motion, i.e., the variability of the heartbeat frequency and the coupling between the motion components, is addressed. All the presented methods are real-time-compatible,

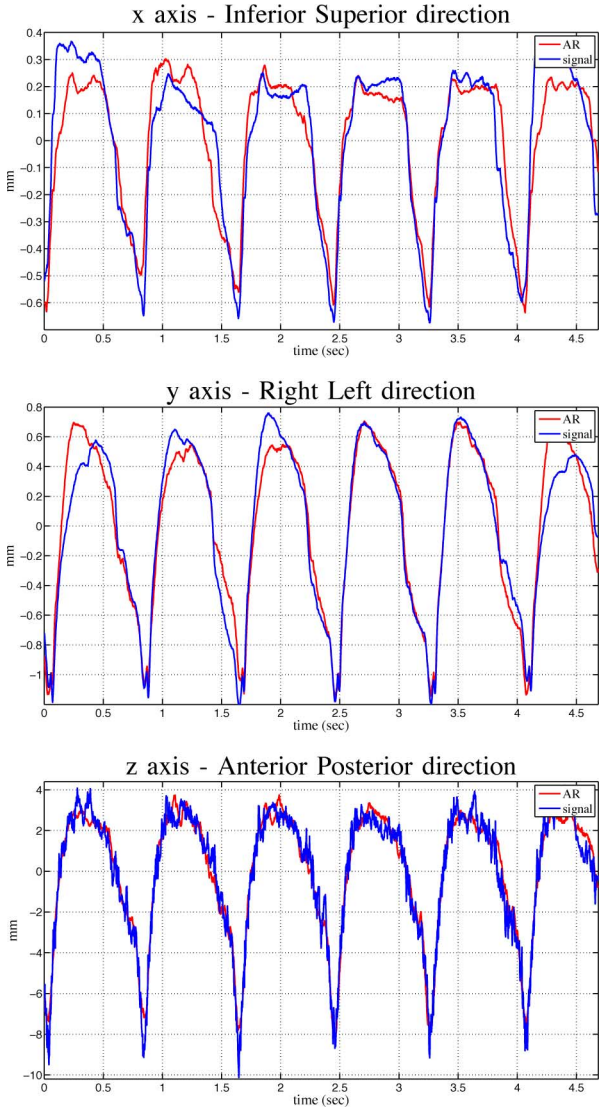

Fig. 6. First datasetone heartbeat period ahead prediction of the cardiac motion for the AR method: only the heartbeat component is reported.

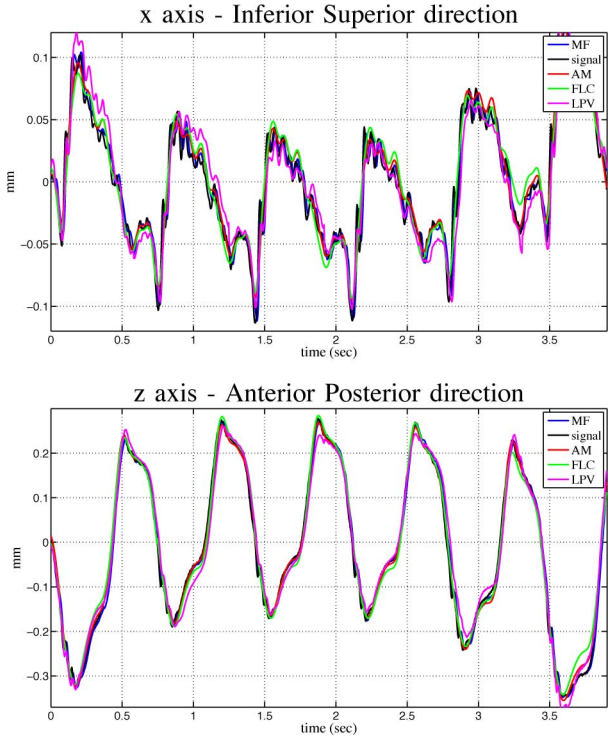

Fig. 7. Second datasetone heartbeat period ahead prediction of the motion components.

so the calculation time issue is not addressed in this section. Table III summarizes the main aspects of the discussion.

A. User Point of View

1) Prediction Accuracy: Even though FLC and AM methods use the same Fourier series framework, we can note that the AM approach improves the results obtained using the FLC algorithm. We also remark that the MF and AM approaches give the best results for the two datasets. The LPV method is efficient only on the first dataset. This is due to a bad extraction of the respiratory component. Indeed, the extraction of the respiratory component has a better signal to noise ratio (SNR) in the first dataset, corresponding to a free cardiac motion, than in the second where the heart is constrained. The LPV method, designed for the prediction of free heart motion, seems to be not suited for a stabilization context.

2) Tuning Simplicity: The simplest methods with respect to parameters tuning are the frequency-domain-based ones, i.e., the FLC and AM methods. Indeed, a simple spectral analysis allows the choice of the number of significant harmonics. Moreover, the number of parameters is not affected by the sampling period. For such methods, one could expect a fully automated estimation of these parameters, so that the prediction can be performed in a few seconds without manual tuning. The LPV method is also easy to tune. Indeed, once the spline model of the respiratory component is identified, the number of parameters to model the heartbeat component equals twice the number of samples of a heartbeat period. For the AR method, a clue has been given to tune the AR filter order. Indeed, the authors propose that the filter order equals to twice the number of significant harmonics. This rule gives quite good results when the data are not noisy. However, with noisy data, the filter order must be increased and several trials are needed to obtain a good tuning. The tuning of the model-free approach is not intuitive because the characteristics of the embedding vector and the storage memory size, which have to be chosen, are not directly related to the heart motion properties. However, as proposed in [16], ten respiratory periods is a good compromise for the storage memory size. Choosing the embedding vector characteristics needs only a few trial-and-error tests because the results are not very sensitive to these parameters, as argued in [29].

B. Algorithm Features

1) Heartbeat Frequency Variation: All the presented methods can take into account a slight change in the heartbeat

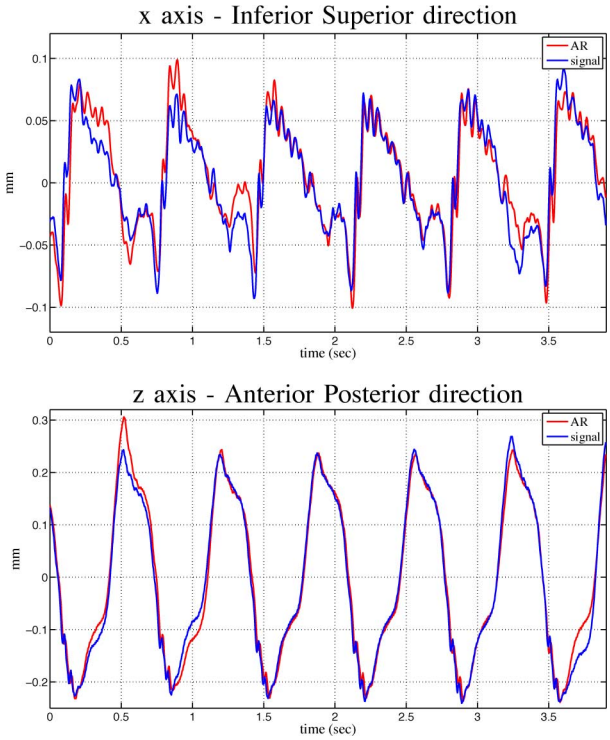

Fig. 8. Second datasetone heartbeat period ahead prediction of the cardiac motion for the AR method: only the heartbeat component is reported.

TABLE III
SUMMARY OF DISCUSSION

	FLC	AR	LPV	MF	AM
Accuracy	+	-	+	++	++
Tuning simplicity	++	-	+	+	++
Heartbeat frequency variation	++	++	-	- -	++
Coupling between the 2 components	- -	+	++	++	++

++: Very good; +: good; -: insufficient; - -: very insufficient.

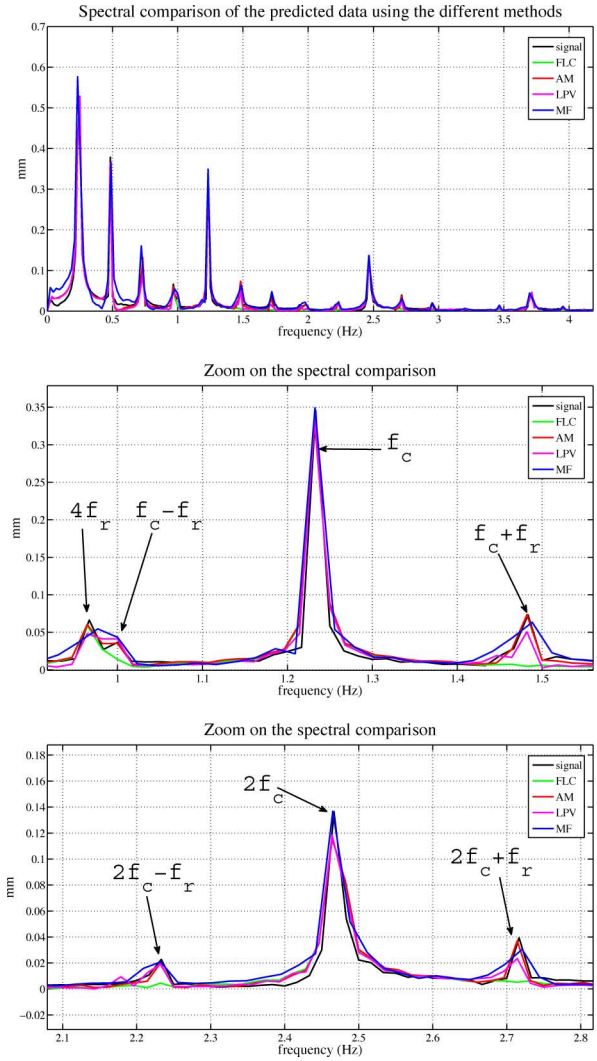

Fig. 9. Spectral analysis of the predicted motion, except for the AR method, with respect to the measured signal (first dataset, motion in the IS direction).

frequency. For the FLC and AM methods, the cardiac frequency is updated online using the ECG signal. The Fourier coefficients are also updated at each sample. The ability of the FLC-like methods to handle the heartbeat frequency variation is assessed in [28]. For the AR model, the filter parameters can also vary to fit a new model if the heartbeat frequency varies. However, more computational burden is necessary for the LPV method to take into account such a variation. The MF approach would also take into account a change in the cardiac frequency, but only a long time after the occurrence of the variation. Indeed, the memory used to construct the past embedding vectors (almost ten respiratory periods) should be completely updated using the new measurements in order to take into account the new cardiac frequency.

2) Coupling Between the Two Components of Heart Motion: Among the frequency-domain-based methods, the FLC approach does not take into account the coupling between the respiratory and the heartbeat components. The AM approach extends the FLC algorithm by considering the influence of the ventilation on the heartbeat component. Note that the coupling could be handled in a better way by the AM method if the linearization constraint was relaxed.

The temporal models have been designed to overcome the main limitation of the FLC method, i.e., considering that the heartbeat and the ventilation components are totally independent. Different degrees of modeling of the coupling can be found. The most relevant approach is the LPV algorithm [17]. The authors assess the coupling between the two motion components and try to model it precisely. The AR method can take into account this coupling if the filter order is chosen adequately.

The MF approach does not involve any modeling of the heart motion and seeks for the best prediction by using the past motion. In that sense, we can argue that this approach takes into account the coupling even without expressing it explicitly.

Fig. 9 shows the spectra of the predicted data (except for the AR method) and the measured motion for the x-direction of the first dataset. This spectral plot outlines that the LPV, MF, and AM approaches handle the coupling between the two heart motion components. Note that the figure also shows that the FLC does not take into account the coupling: the peaks of the

measured signal at $f_c - f_r$ and $f_c + f_r$ are, for instance, not observed for the predicted signal.

In conclusion, the proposed AM method gives promising results when compared to the existing approaches. It takes into account two features that seem of great importance for cardiac surgery: the adaptation to heartbeat frequency variation and the modeling of the coupling between the two heart motion components. Moreover, the AM algorithm is easy to tune and implement.

VII. Conclusion

In this paper, a detailed review and a classification of the main heart motion-prediction algorithms have been provided with emphasis on the modeling aspects of the different approaches. We particularly highlighted a novel prediction method based on AM. Experimental results using two different *in vivo* datasets were also given to evaluate the accuracy of the most relevant approaches before discussing their main properties. The AM algorithm gives promising results.

Future work includes the use of the AM technique in a predictive control scheme. The obtained control law will be used in the controller of the active cardiac stabilizer proposed in [15]. This will allow us to evaluate the robustness of the prediction method with respect to physiological parameter variations in a cardiac stabilization context.

Appendix A

Least-Squares-Algorithm With Forgetting Factor

If the data samples at each time k can be expressed as

$$y(k) = \psi(k)^T \ \theta(k-1) \tag{46}$$

where $\psi(k)$ is a known regression vector and θ is the parameter vector to be estimated, which can be estimated online using the following RLS algorithm with a forgetting factor λ [30]:

$$\begin{aligned}
\hat{y}(k) &= \psi(k)^T \, \hat{\theta}(k-1) \\
K(k) &= \frac{P(k-1)\psi(k)}{\lambda + \psi(k)^T P(k-1)\psi(k)} \\
\hat{\theta}(k) &= \hat{\theta}(k-1) + K(k)(y(k) - \hat{y}(k)) \\
P(k) &= \frac{1}{\lambda}\left(P(k-1) - \frac{P(k-1)\psi(k)\psi(k)^T P(k-1)}{\lambda + \psi(k)^T P(k-1)\psi(k)}\right)
\end{aligned} \tag{47}$$

where $K(k)$ is the correction gain vector and $P(k)$ is the covariance matrix. The variables $\hat{\theta}(k)$ and $\hat{y}(k)$ denote the estimate at sample k of $\theta(k)$ and $y(k)$, respectively.

References

[1] W. D. Boyd, N. D. Desai, D. F. D. Rizzo, R. J. Novick, F. N. McKenzie, and A. H. Menkis, "Off-pump surgery decreases post-operative complications and resource utilization in the elderly," *Ann. Thorac. Surg.*, vol. 68, pp. 1490–1493, 1999.

[2] D. Van Dijk, E. Jansen, R. Hijman, A. Nierich, J. Diephuis, K. Moons, J. Lahpor, C. Borst, A. Keizer, H. Nathoe, D. Grobbee, P. De Jaegere, and C. Kalkman, "Cognitive outcome after off-pump and on-pump coronary artery bypass graft surgery," *J. Amer. Med. Assoc.*, vol. 287, no. 11, pp. 1405–1412, 2002.

[3] M. Mack, "Pro: Beating-heart surgery for coronary revasculation: Is it the most important development since the introduction of the heart-lung machine?" *Ann. Thorac. Surg.*, vol. 70, no. 5, pp. 1767–1797, 2000.

[4] M. Lemma, A. Mangini, A. Redaelli, and F. Acocella, "Do cardiac stabilizers really stabilize? Experimental quantitative analysis of mechanical stabilization," *Interactive Cardiovasc. Thorac. Surg.*, vol. 4, no. 3, pp. 222–226, 2005.

[5] P. Cattin, H. Dave, J. Grunenfelder, G. Szekely, M. Turina, and G. Zund, "Trajectory of coronary motion and its significance in robotic motion cancellation," *Eur. J. Cardio-Thorac. Surg.*, vol. 25, no. 5, pp. 786–790, 2004.

[6] D. Loisance, K. Nakashima, and M. Kirsch, "Computer-assisted coronary surgery: Lessons from an initial experience," *Interactive Cardiovasc. Thorac. Surg.*, vol. 4, pp. 398–401, 2005.

[7] U. Kappert, R. Cichon, J. Schneider, V. Gulielmos, T. Ahmadzade, J. Nicolai, S.-M. Tugtekin, and S. Schueler, "Technique of closed chest coronary artery surgery on the beating heart," *Eur. J. Cardio-Thorac. Surg.*, vol. 20, pp. 756–769, 2001.

[8] A. Thakral, J. Wallace, D. Tolmin, N. Seth, and N. Thakor, "Surgical motion adaptive robotic technology (S.M.A.R.T): Taking the motion out of physiological motion," in *Proc. Int. Conf. Med. Image Comput. Comput.-Assisted Intervention* (Lecturer Notes in Computer Science, vol. 2208), pp. 317–325, 2001.

[9] S. Jacobs, D. Holzhey, F. Mohr, and V. Falk, "Limitations for manual and telemanipulator-assisted motion tracking and dexterity for endoscopic surgery," in *Proc. Int. Congr. Comput.-Assisted Radiol. Surg.*, vol. 1256, pp. 673–677, 2003.

[10] A. Trejos, S. Salcudean, F. Sassani, and S. Lichtenstein, "On the feasibility of a moving support for surgery on the beating heart," in *Proc. Int. Conf. Med. Image Comput. Comput.-Assisted Intervention* (Lecturer Notes in Computer Science, vol. 1679), pp. 1088–1097, 1999.

[11] Y. Nakamura, K. Kishi, and H. Kawakami, "Heartbeat synchronization for robotic cardiac surgery," in *Proc. IEEE Int. Conf. Robot. Autom.*, 2001, vol. 2, pp. 2014–2019.

[12] R. Ginhoux, J. Gangloff, M. de Mathelin, L. Soler, M. Sanchez, and J. Marescaux, "Active filtering of physiological motion in robotized surgery using predictive control," *IEEE Trans. Robot.*, vol. 21, no. 1, pp. 67–79, Feb. 2005.

[13] O. Bebek and M. Cavusoglu, "Intelligent control algorithms for robotic-assisted beating heart surgery," *IEEE Trans. Robot.*, vol. 23, no. 3, pp. 468–480, Jun. 2007.

[14] N. Patronik, M. Zenati, and C. Riviere, "Preliminary evaluation of a mobile robotic device for navigation and intervention on the beating heart," *Comput.-Aided Surg.*, vol. 10, no. 5, pp. 225–232, 2005.

[15] W. Bachta, P. Renaud, E. Laroche, J. Gangloff, and A. Forgione, "Cardiolock: An active cardiac stabilizer—First in vivo experiments using a new robotized device," in *Proc. Int. Conf. Med. Image Comput. Comput.-Aided Intervention* (Lecturer Notes in Computer Science, vol. 4791), pp. 78–85, 2007.

[16] T. Ortmaier, M. Groger, D. Boehm, V. Falk, and G. Hirzinger, "Motion estimation in beating heart surgery," *IEEE Trans. Biomed. Eng.*, vol. 52, no. 10, pp. 1729–1740, Oct. 2005.

[17] L. Cuvillon, J. Gangloff, M. de Mathelin, and A. Forgione, "Toward robotized beating heart TECABG: Assessment of the heart dynamics using high-speed vision," in *Proc. Int. Conf. Med. Image Comput. Comput.-Assisted Intervention* (Lecturer Notes in Computer Science, vol. 3750), pp. 551–558, 2005.

[18] T. Franke, O. Bebek, and C. Cavusoglu, "Improved prediction of heart motion using an adaptive filter for robot assisted beating heart surgery," in *Proc. IEEE/RSJ Int. Conf. Intell. Robots Syst.*, 2007, pp. 509–515.

[19] W. Bachta, E. Laroche, P. Renaud, and J. Gangloff, "Active cardiac stabilization using h infinity control methodology," presented at the IFAC World Congr., Seoul, Korea, 2008.

[20] G. Shechter, J. Resar, and E. McVeigh, "Displacement and velocity of the coronary arteries: Cardiac and respiratory motion," *IEEE Trans. Med. Imag.*, vol. 25, no. 3, pp. 369–375, Mar. 2006.

[21] D. Oberkampf, D. DeMenthon, and L. Davis, "Iterative pose estimation using coplanar feature points," *CVGIP: Image Understanding*, vol. 63, no. 3, pp. 495–511, 1996.

[22] P. Hunter, A. Pullan, and B. Smaill, "Modeling total heart function," *Annu. Rev. Biomed. Eng.*, vol. 5, pp. 147–177, 2003.

[23] M. Sermesant, H. Delingette, and N. Ayache, "An electromechanical model of the heart for image analysis and simulation," *IEEE Trans. Med. Imag.*, vol. 25, no. 5, pp. 612–625, May 2006.
[24] F. Takens, "Detecting strange attractors in turbulence," *Lect. Notes Math.*, vol. 898, pp. 366–381, 1981.
[25] T. Franke, O. Bebek, and M. Cavusoglu, "Prediction of heartbeat motion with a generalized adaptive filter," in *Proc. IEEE Int. Conf. Robot. Autom.*, 2008, pp. 2916–2921.
[26] C. Riviere, R. Rader, and N. Thakor, "Adaptive canceling of physiological tremor for improved precision in microsurgery," *IEEE Trans. Biomed. Eng.*, vol. 45, no. 7, pp. 839–846, Jul. 1998.
[27] M. Bodson and S. Douglas, "Adaptive algorithms for the rejection of sinusoidal disturbances with unknown frequency," *Automatica*, vol. 33, no. 12, pp. 2213–2221, 1997.
[28] S. Yuen, P. Novotny, and R. Howe, "Quasiperiodic predictive filtering for robot-assisted beating heart surgery," in *Proc. IEEE Int. Conf. Robot. Autom.*, 2008, pp. 3875–3880.
[29] T. Ortmaier, "Motion compensation in minimally invasive robotic surgery," Ph.D. dissertation, Tech. Univ. München, Munich, Germany, 2002.
[30] G. Goodwin and K. Sin, *Adaptive Filtering Prediction and Control*. Englewood Cliffs, NJ: Prentice-Hall, 1984.
[31] L. Ljung, "Recursive identification algorithms," *Circuits Syst. Signal Process.*, vol. 21, no. 1, pp. 57–68, 2002.
[32] A. McQuarrie and C. Tsai, *Regression and Time Series Model Selection*. Singapore: World Scientific, 1998.
[33] C. de Boor, *A Practical Guide to Splines*. New York: Springer-Verlag, 1978.

Wael Bachta graduated in control systems engineering from the Ecole Nationale Supérieure de Physique de Strasbourg, Strasbourg, France, in 2005, and received the M.S. and Ph.D. degrees in robotics from the University Louis Pasteur, Strasbourg, in 2005 and 2008, respectively.

He is currently a Lecturer at Strasbourg University, Strasbourg, where he is a member of the EAVR (Control Vision and Robotics) Group at the Laboratoire des Sciences de l'Image, de l'Informatique et de la Télédétection. His current research interests include medical robotics, visual servoing, and mechatronics.

Dr. Bachta was a recipient of the 2007 Young Scientist Award in "Computer-Assisted Intervention Systems and Robotics" at the Medical Image Computing and Computer Assisted Intervention (MICCAI) Conference.

Pierre Renaud received the M.Sc. degree in mechanics and materials from the Ecole normale supéérieure de (ENS) Cachan, Paris, France, in 2000, and the Ph.D. degree in robotics from Clermont-Ferrand University, Clermont-Ferrand, France.

Since 2004, he has been an Associate Professor at the National Institute of Applied Science (INSA) of Strasbourg, France. He is also a member of the EAVR (Control Vision and Robotics) Team at the Laboratoire des Sciences de l'Image, de l'Informatique et de la Télédétection, University of Strasbourg, Strasbourg. His current research interests include medical robotics, robot design, parallel robots, and mechatronics.

Loïc Cuvillon graduated in control systems engineering from the Ecole Nationale Supérieure de Physique de Strasbourg, Strasbourg, France, in 2002, and the M.S. and Ph.D. degrees in robotics from the University Louis Pasteur, Strasbourg, in 2002 and 2006, respectively.

Since 2007, he has been a Maître de Conférences at Strasbourg University, where he is a member of the EAVR (Control Vision and Robotics) Team at the Laboratoire des Sciences de l'Image, de l'Informatique et de la Télédétection. His current research interests include visual servoing of robotic manipulators, control of flexible structures, and medical robotics.

Edouard Laroche was born in 1971. He graduated from the Ecole Nationale Supérieure d'Electricité et de Mécanique, Nancy, France, in 1994, and the Agrégation degree in electrical engineering and the Ph.D. degree from the Ecole Normale Supérieure de Cachan, Paris, France, in 1995 and 2000, respectively.

He is currently a Full Professor at the University of Strasbourg, Strasbourg, France. He is affiliated with the Laboratoire des Sciences de l'Image de l'Informatique et de la Télédétection (Unitee Mixte de Recherche Centre national de la recherche scientifique 7005). His current research interests include robustness issues in identification and control of electromechanical systems.

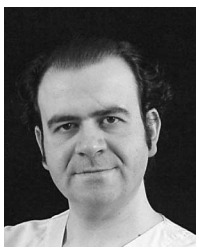

Antonello Forgione graduated in medicine from the University of Naples, Naples, Italy, in 1996, and the Ph.D. degree in new technologies applied to general and oncologic surgery from the Federico II University, Naples, in 2006.

During 2003, he was engaged in specialization in digestive and endoscopic surgery. From 2003 to 2007, he was a Research Fellow at the European Institute of Tele-Surgery (IRCAD)/European Institute of Telesurgery (EITS). He is currently a Consultant Surgeon in general surgery at Niguarda C Granda Hospital, Milan, Italy, where he is the Scientific Director of the Advanced International Mini-Invasive Surgery (AIMS) Academy. His current research interests include miniinvasive surgery, robotic and microrobotic manipulators, and virtual and augmented reality.

Dr. Forgione received a prize as one of the world's leading researchers in the filed of miniivasive surgery during the World Congress of Surgery, Yokohama, Japan, in 2008.

Jacques Gangloff (M'96) graduated from the Ecole Normale Supérieure de Cachan, Paris, France, in 1995, and the M.S. and Ph.D. degrees in robotics from the University Louis Pasteur, Strasbourg, France, in 1996 and 1999, respectively.

Between 1999 and 2005, he was an Associate Professor at the University of Strasbourg, where he became a Professor in 2005, and is currently a member of the EAVR (Control Vision and Robotics) Team at the Laboratoire des Sciences de l'Image, de l'Informatique et de la Télédétection (LSIIT). His current research interests include visual servoing, predictive control, and medical robotics.

Prof. Gangloff was a recipient of the Best Vision Paper Award at the IEEE International Conference on Robotics and Automation (ICRA 2004) and the 2005 Best Paper Award of the IEEE TRANSACTIONS ON ROBOTICS AND AUTOMATION.